

k/k_0 . This becomes barely discernible for 10^{-1} and the spectrum has a smooth roll off for 10^0 . Within the regime $k_0 r_0 \ll 10^{-1}$ and $kr_0 \ll 1$, k scales with respect to k_0 . In Fig. 2, when $k_0 r_0 \geq 10^2$, we obtain a $\exp(-k^2 r_0/2k_0)$ decay and similarity with respect to the variable $(r_0/2k_0)^{1/2}$, pointing out the significance of the geometric mean of the two scale lengths. For earlier times or smaller $k_0 r_0$ values, or even for large $k_0 r_0$ but k greater than k_0 , one finds that the spectrum decreases at a slower rate with respect to wave number. A similar behavior is illustrated by Deissler^{8,9} on the approach to the final stage.

This example shows that our analytic model can provide plausible theoretical variations for intermediate stages of decay, given theoretical predictions on the initial or late period. It also is useful to match to experimental data, which may not be representative of either the initial or final stages.

References

- ¹ Shkarofsky, I. P., "Generalized Turbulence Space-Correlation and Wave Number-Spectrum Function Pairs," *Canadian Journal of Physics*, Vol. 46, No. 19, Oct. 1968, pp. 2133-2153.
- ² Tatarski, V. I., *Wave Propagation in a Turbulent Medium*, McGraw-Hill, New York, 1961, p. 138.
- ³ Hinze, J. O., *Turbulence*, McGraw-Hill, New York, 1959, Chap. 3.
- ⁴ Batchelor, G. K., *The Theory of Homogeneous Turbulence*, Cambridge University Press, Cambridge, 1956, Chaps. 5-7.
- ⁵ Kolmogorov, A. N., "The Local Structure of Turbulence in Incompressible Viscous Fluid for Very Large Reynolds Numbers," *Doklady Akademii Nauk, USSR*, Vol. 30, 1941, p. 301.
- ⁶ Saffman, P. G., "Note on Decay of Homogeneous Turbulence," *The Physics of Fluids*, Vol. 10, No. 6, June 1967, p. 1349.
- ⁷ Saffman, P. G., "The Large-Scale Structure of Homogeneous Turbulence," *Journal of Fluid Mechanics*, Vol. 27, Pt. 3, Feb. 24, 1967, pp. 581-593.
- ⁸ Deissler, R. G., "A Theory of Decaying Homogeneous Turbulence," *The Physics of Fluids*, Vol. 3, No. 2, March-April 1960, pp. 176-187.
- ⁹ Deissler, R. G., "On The Decay of Homogeneous Turbulence Before the Final Period," *The Physics of Fluids*, Vol. 1, No. 2, March-April 1958, pp. 111-121.

Reflection of a Shock Wave into a Density Gradient

RONALD K. HANSON* AND DONALD BAGANOFF†
Stanford University, Stanford, Calif.

1. Introduction

RECENT studies of normal shock-wave reflection in a relaxing gas (e.g., in a shock tube) have shown that the flowfield behind the reflected shock wave is spatially non-uniform even after steady-state conditions are attained.^{1,2} The region containing this nonuniform gas has been termed an entropy layer, and the reasons for its existence are linked to the nonsteady nature of the reflection process which occurs when a shock wave reflects into a nonuniform flow. While the aforementioned papers have dealt with the technically important cases of vibrational and chemical relaxation, the solutions have required lengthy numerical calculations. It

Received June 16, 1969; revision received November 17, 1969. This work was performed under the support of NASA Grant NGR 05-020-245.

* Research Associate, Department of Aeronautics and Astronautics; now a NRC Postdoctoral Fellow at NASA Ames Research Center, Moffett Field, Calif. Member AIAA.

† Assistant Professor, Department of Aeronautics and Astronautics. Member AIAA.

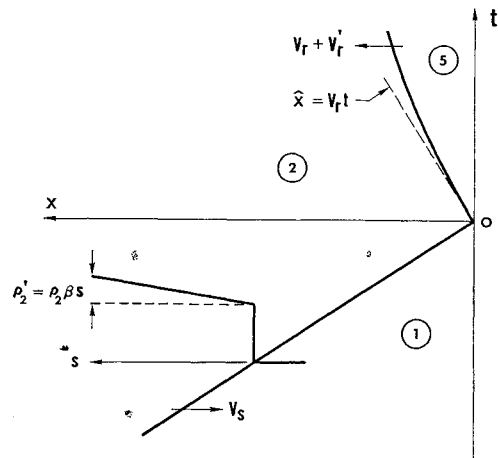


Fig. 1 Space-time diagram for shock-wave reflection.

is appropriate, therefore, to study a simpler case of nonsteady shock reflection which, although retaining many of the physical features of more complicated problems, lends itself to an analytical solution.

The object of this note is to present an analysis for a simple but illustrative case of shock-wave reflection in which the flow behind the incident shock wave exhibits a linear density variation and the gas is everywhere ideal. The density variation is assumed small so that all quantities behind both the incident and reflected shock waves vary only slightly from their unperturbed values, and linearized equations can be used to calculate the flowfield.

A previous analysis which also dealt with the effects of nonuniformities behind the incident shock wave was presented by Rudinger.³ However, his analysis was tailored specifically for the case wherein the nonuniformities resulted from the formation of a side-wall boundary layer. Furthermore, his results were restricted to weak shock waves ($M_s < 2$), and he did not allow for variations in the velocity of the reflected shock wave or for gradients in the entropy behind either the incident or reflected shock waves.

2. Analysis

The space-time diagram representing the over-all flow process is shown in Fig. 1, where x is the distance from the shock-tube end wall and t is the time after reflection. The density perturbation will be represented by

$$\rho'_2/\rho_2 = \beta s \quad (1)$$

where ρ_2 is the unperturbed value of the density, β is a density-gradient parameter, and s is the distance behind the incident shock wave.

For a given density distribution, the variations in the values of other thermodynamic properties are determined by the conservation equations of mass and momentum and the thermal equation of state. For example, since the pressure behind a constant-speed incident shock wave (in a constant area duct) is given by

$$p_2 = p_1 + \rho_1 V_s^2 (1 - \rho_1/\rho_2)$$

then the perturbation in pressure owing to a small variation in density is

$$p'_2 = \rho_1 V_s^2 (\rho_1/\rho_2) (\rho'_2/\rho_2)$$

If one neglects p_1 in the previous equation ($p_1 \ll p_2$ for moderately strong shock waves), the last equation can be rewritten in dimensionless form as

$$p'_2/p_2 = \beta s / (\rho_{21} - 1) \quad (2)$$

where the abbreviated notation $\rho_{21} = \rho_2/\rho_1$ has been adopted. Note that the energy conservation equation has not been

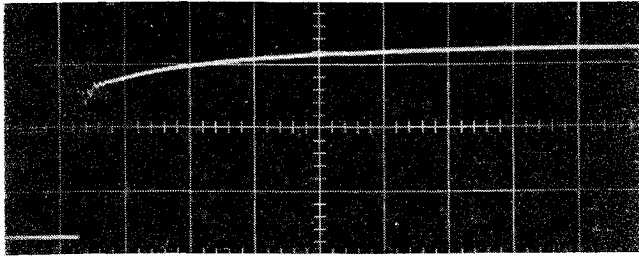


Fig. 2 End-wall pressure history for shock-wave reflection in vibrationally relaxing N_2 . Shock speed is 2.9 mm/ μ sec, initial pressure is 10 torr, and sweep speed is 1 μ sec/div.

utilized, and in fact the specification of a changing density implies nonadiabatic flow. The justification for this approach follows from the importance of the density in determining the character of the flow in the reflected-shock region.

The boundary conditions for the flow in region 5 are determined from the standard shock-jump relations. For example, retaining only first-order terms in the perturbed quantities, one finds that

$$\hat{\rho}'_5/\rho_5 = \hat{\rho}'_2/\rho_2 + \hat{\rho}'_{s2}/\rho_{s2} = \hat{\rho}'_2/\rho_2 + (4/G)(M'_r/M_r)$$

where M_r (the Mach number of the reflected shock wave) is defined by

$$M_r = [V_r + V_s(1 - \rho_{12})]/a_2$$

and

$$G = (\gamma - 1)M_r^2 + 2$$

The caret symbol has been used to denote the value of a quantity along the reflected-shock trajectory. The perturbation in the reflected-shock Mach number results from variations in ρ_2 , a_2 , and V_r . However, the variations in a_2 and ρ_2 are related so that the perturbation in Mach number becomes

$$M'_r/M_r = H(\hat{\rho}'_2/\rho_2) + \rho_{25}(V'_r/V_r)$$

where H is defined by

$$H = V_s/\rho_{21}a_2M_r + (\rho_{21} - 2)/2(\rho_{21} - 1)$$

Consistent with the use of first-order perturbation theory, the jump conditions across the reflected shock wave can be satisfied along the unperturbed shock trajectory. The perturbed values for the flow properties immediately upstream of the reflected shock wave are thus given simply by substituting $s = (V_r + V_s)t$ into the appropriate equations for the flow properties in region 2. Using Eq. (1), the density perturbation becomes

$$\hat{\rho}'_5(t) = [\rho_5(1 + 4H/G)]Lt + [4\rho_2/GV_r]V'_r = ALt + BV'_r \quad (3)$$

where $Lt = \beta(V_r + V_s)t$. Similar analyses for pressure and particle velocity yield the boundary conditions

$$\frac{\hat{p}'_5(t)}{\rho_5 a_5} = \left[\frac{4M_r^2 H a_5}{\rho_{s2}(\gamma + 1)} + \frac{a_5}{\gamma(\rho_{21} - 1)} \right] Lt + \left[\frac{4M_r a_{s2}}{\rho_{s2}(\gamma + 1)} \right] \times V'_r = CLt + DV'_r \quad (4)$$

and

$$\hat{u}'_5(t) = [4HV_r/G - V_s/\rho_{s1}]Lt + [1 + \rho_{25}(4/G - 1)]V'_r = ELt + FV'_r \quad (5)$$

The flowfield in region 5 is found by solving the elementary wave equation in the perturbed variables p'_5 and u'_5 , e.g.,

$$\partial^2 p'_5 / \partial t^2 - a_5^2 \partial^2 p'_5 / \partial x^2 = 0 \quad (6)$$

(Note, for this problem, that one cannot utilize an elementary wave equation in either of the perturbed variables ρ'_5 or T'_5 . This is a result of the fact that the entropy varies between adjacent particle paths in region 5; i.e., the flow is nonhomotropic). After applying the no-flow boundary condition at the end wall and the boundary conditions along the unperturbed shock trajectory, one can show that the perturbed velocity and pressure distributions are

$$u_5/V_r = -KLx/V_r = -(Kx/\hat{x})Lt \quad (7)$$

and

$$p'_5/p_5 = (\gamma K)Lt \quad (8)$$

where

$$K = (FC - DE)/(Fa_5 + DV_r)$$

The quantity $\hat{x} = V_r t$ was introduced in Eq. (7) in order to provide a common form with the solutions shown below where \hat{x} appears as a natural variable. The perturbation in the reflected-shock velocity is given by

$$V'_r/V_r = -JLt \quad (9)$$

where

$$J = (C + Ea_5/V_r)/(DV_r + Fa_5)$$

The density distribution, established by integrating the continuity equation and satisfying the boundary condition for ρ'_5 at the shock wave, is

$$\rho'_5/\rho_5 = [K + I(x/\hat{x})]Lt \quad (10)$$

where

$$I = (1 + 4H/G - 4J/G\rho_{s2} - K)$$

Using the linearized equation of state, one can now show that the temperature distribution is given by

$$T'_5/T_5 = [(\gamma - 1)K - I(x/\hat{x})]Lt \quad (11)$$

while the entropy perturbation becomes

$$S'_5/R = -[\gamma IL/(\gamma - 1)V_r]x \quad (12)$$

Calculations of the dimensionless coefficients I , J , and K show only small variations for $M_s > 3$ and therefore one can approximate them with constants. For $\gamma = \frac{7}{5}$, those constants are 0.70, 0.90, and 0.54 for I , J , and K , respectively; for $\gamma = \frac{5}{3}$, the constants are 0.73, 0.73, and 0.45, respectively.

3. Discussion of Results

An inspection of Eq. (7) shows that the velocity perturbation is a function of x only; the negative sign indicates that the motion is toward the end wall. The pressure perturbation, on the contrary, is not a function of x , and it rises uniformly with time for all the fluid particles in region 5. It is of interest that, for either a monatomic or diatomic gas, the pressure perturbation p'_5/p_5 is nearly 8% at the instant the reflected shock wave intercepts a density variation $\hat{\rho}'_2/\rho_2$ of 10%. This last result is physically reasonable when one recognizes that any density increase in region 2 represents a proportionate increase in dynamic pressure as seen by the reflected shock wave, and hence a similar increase in static pressure must arise in region 5.

The solution for the reflected-shock speed indicates a perturbation which is negative and proportional to time. However, the Mach number with respect to the incident flow actually increases because of the decreasing value of the speed of sound in region 2. The result of the increasing shock strength, and of the increasing value of mass density in region 2, is the development of a large positive perturbation in density immediately behind the reflected shock wave. Owing

to compressive effects, the density perturbation at the end wall also increases with time, but at a slower rate than the perturbation at the shock wave. The unsteady reflection process thus creates a negative gradient in density toward the end wall.

An examination of Eq. (11) shows that the temperature perturbation just behind the reflected shock front is negative and becomes more negative with time, whereas the perturbation at the end wall is positive and increases with time. In fact, there is a growing region of gas near the end wall, of width $[(\gamma - 1)K/I]\bar{x}$, wherein the temperature perturbation is positive and increases steadily with time.

This unexpected result for the temperature can be explained as follows. Implicit in the conservation equations for steady, one-dimensional flow of an ideal gas is the requirement that the flow in region 2 lose thermal energy in order for the density to increase. This energy loss is responsible for the negative temperature perturbation immediately behind the reflected shock wave. Whatever the mechanism for energy extraction from region 2, the momentum of this gas is increased, and this increase in momentum manifests itself as a pressure rise in region 5. The net effect is that compressive work is continually being done on the gas in region 5, thus adding thermal energy along each particle path. Furthermore, the rate of energy addition is the same along all particle paths since the pressure rises uniformly. The energy of a particular gas element at any given time thus depends on the initial thermal energy of the element upon entering region 5 and the length of time spent in region 5.

Some of the results obtained here for an ideal gas are of use in understanding the shock-reflection process when density gradients are present in nonideal gases. Although the numerical results may differ, many of the important physical concepts are retained. For example, one must conclude that radiative cooling behind an incident shock wave, a nonadiabatic effect which would increase the density in region 2, should also cause an entropy layer. If radiative cooling occurs in region 2, one may thus expect a trend toward higher temperatures near the end wall and lower temperatures near the reflected shock wave. In a real case, of course, when energy is being lost by means of radiation from region 2, region 5 may also be losing energy, and this fact would have to be included in any meaningful calculation.

Since vibrational and chemical relaxation cause a density increase behind the incident shock wave, the present model also accounts for the principal features of reflected-shock flowfields in relaxing gases. This connection is possible since relaxation effects in region 5 may be considered part of the reflected-shock structure (owing to the comparatively fast relaxation at the higher temperature and density of region 5). One would thus expect entropy layers with positive temperature perturbations and negative density perturbations near the end wall.^{1,2}

For cases involving relaxation, only a limited density change occurs in region 2 so the resulting perturbations in region 5 eventually approach a steady-state distribution. This limiting behavior is clearly exhibited in Fig. 2, which presents a measurement of the pressure on a shock-tube end wall during the reflection process in vibrationally relaxing nitrogen.⁴ The sharp rise in pressure corresponds to the arrival of the shock wave at the end wall while the subsequent gradual rise in pressure represents the perturbation caused by the relaxation in region 2.

After steady-state conditions are reached, the reflected shock moves away from the end wall at a steady speed, leaving behind a growing region of gas with a uniform equilibrium state and a stationary entropy layer adjacent to the end wall. The thickness of such an entropy layer scales directly with the length of the incident-shock relaxation zone, and is essentially that relaxation length compressed by the density ratio across the reflected shock wave.

References

- ¹ Johannesen, N. H., Bird, G. A., and Zienkiewicz, H. K., "Theoretical and Experimental Investigations of the Reflection of Normal Shock Waves with Vibrational Relaxation," *Journal of Fluid Mechanics*, Vol. 30, Pt. 1, 1967, pp. 51-64.
- ² Presley, L. L. and Hanson, R. K., "Numerical Solutions of Reflected Shock-Wave Flowfields with Nonequilibrium Chemical Reactions," *AIAA Journal*, Vol. 7, No. 12, Dec. 1969, pp. 2267-2273.
- ³ Rudinger, G., "Effect of Boundary-Layer Growth in a Shock Tube on Shock Reflection From a Closed End," *The Physics of Fluids*, Vol. 4, 1961, pp. 1463-1473.
- ⁴ Hanson, R. K., "An Experimental and Analytical Investigation of Shock-Wave Reflection in a Relaxing Gas," SUDAAR 345, May 1968, Stanford Univ., Stanford, Calif.

Computation of Current Sheet Speeds in Plasma Accelerators

R. J. WOLF*

AND

F. Y. SORRELL†

University of Colorado, Boulder, Colo.

AND

Y. NAKAGAWA‡

National Center for Atmospheric Research, Boulder, Colo.

WHEN it is desired to produce very high current sheet speeds in plasma accelerators, it is usually necessary to use very large currents. To obtain these currents the external circuit inductance is usually reduced as much as practical and generally results in a condition where the accelerator inductance and its time change govern the drive current, rather than the external circuit. In order to investigate this we have used the snowplow¹ model to give the current sheet position and a circuit equation that assumes a fixed external circuit inductance in series with a time dependent inductance (the accelerator). No circuit resistance is included. This technique has been used previously² and thus the purpose of this Note is not to introduce the computation technique, but to present some new and useful results.

We wish to use this technique to compute the speed of the current sheet in a coaxial accelerator, and in this device the force on the current sheet varies with the radius squared. Thus, one must either apply the snowplow model at some mean radius, or, as was done here, apply the equations at several radii. To do this, a separate momentum balance is made at each of 5 equally spaced radii and the position of the current layer is computed at each radius. This will give a parabolic shaped current sheet which should approximate that found experimentally by Keck³ for this geometry. When this is done the snowplow equation for the distance of the current layer from the insulator of the accelerator, x_i , at the radius r_i is

$$d/dt[\rho_i x_i(dx_i/dt)] = \mu_0 I^2 / 8\pi^2 r_i^2 \quad (1)$$

Received November 10, 1969. This work was supported in part by the National Center for Atmospheric Research and in part by the National Science Foundation grant GK-1202.

* Graduate student, Department of Aerospace Engineering Sciences.

† Assistant Professor, Department of Aerospace Engineering Sciences; now Assistant Professor, Department of Engineering Mechanics, North Carolina State University, Raleigh, N.C.

‡ Physicist, high altitude observatory.